Journal of Geodesy (1997) 71: 189–208

Journal of Geodesy

Long-wavelength global gravity field models: GRIM4-S4, GRIM4-C4

P. Schwintzer[1], Ch. Reigber[1], A. Bode[1], Z. Kang[1], S.Y. Zhu[1], F.-H. Massmann[1], J.C. Raimondo[1], R. Biancale[2], G. Balmino[2], J.M. Lemoine[2], B. Moynot[2], J.C. Marty[2], F. Barlier[3], Y. Boudon[3]

[1] GeoForschungsZentrum (GFZ, Div. I), Telegrafenberg A17 D-14473 Potsdam, Germany

[2] Groupe de Recherche de Géodésie Spatiale (GRGS), 18, Avenue Edouard Belin F-31401 Toulouse Cedex 4, France

[3] Groupe de Recherche de Géodésie Spatiale (GRGS), OCA/CERGA, Avenue Copernic, F-06130 Grasse, France

Received 1 February 1996; Accepted 17 July 1996

Summary. GFZ Potsdam and GRGS Toulouse/Grasse jointly developed a new pair of global models of the Earth's gravity field to satisfy the requirements of the recent and future geodetic and altimeter satellite missions. A precise gravity model is a prerequisite for precise satellite orbit restitution, tracking station positioning and altimeter data reduction. According to different applications envisaged, the new model exists in two parallel versions: the first one being derived exclusively from satellite tracking data acquired on 34 satellites, the second one further incorporating satellite altimeter data over the oceans and terrestrial gravity data. The most recent "satellite-only" gravity model is labelled GRIM4-S4 and the "combined" gravity model GRIM4-C4. The models are solutions in spherical harmonics and have a resolution up to degree and order 60 plus a few resonance terms in the case of GRIM4-S4, and up to degree/order 72 in the case of GRIM4-C4, corresponding to a spatial resolution of 555 km at the Earth's surface. The gravitational coefficients were estimated in a rigorous least squares adjustment simultaneously with ocean tidal terms and tracking station position parameters, so that each gravity model is associated with a consistent ocean tide model and a terrestrial reference frame built up by over 300 optical, laser and Doppler tracking stations. Comprehensive quality tests with external data and models, and test arc computations over a wide range of satellites have demonstrated the state-of-the-art capabilities of both solutions in long-wavelength geoid representation and in precise orbit computation.

1. Introduction

The recovery of the very long-wavelength part of the free air Earth's gravity field, and correlatively the gravitational geopotential and the figure of the Earth, became possible some 30 years ago when precise tracking of near Earth orbiting satellites began. The improvements in tracking accuracy from the early camera observations to modern laser and microwave tracking systems and the growing number of available satellites gradually increased the resolution in global gravity field models to wavelengths of about 1500 km at the Earth's surface. Higher resolution is obtained through a combination of the long-wavelength information, coming from satellite orbit perturbation analyses, with surface data from satellite altimetry over the oceans and gravimetry.

Long-wavelength global gravity field models are subject to geophysical investigations on the mass and density distribution of the Earth's deep interior especially constraining and refining results implied by seismic tomography and plate tectonic motion (e.g. Ricard 1989). The geoid, also called the physical figure of the Earth, is the geometric representation of that surface of equal gravity potential which best coincides with the undisturbed ocean surface. In oceanography the geoid is the reference surface for altimeter derived quasi-stationary sea surface topography models and therewith a prerequisite for studying the geostrophic ocean currents. In geodesy the geoid is the reference surface for the national height systems and digital terrain models at different scales. The long-wavelength information is also essential for regional and local modelling of the geoid fine structure. Precise satellite orbit determination, as employed in satellite altimetry and point positioning, requires most accurate global gravity field models with a resolution demand depending largely on the altitude of the satellite.

Within the well established long-term French-German cooperation in global gravity field modelling a series of so-called GRIM-models has been issued starting with GRIM1 in 1976, then GRIM2 (Balmino et al. 1978) and GRIM3 (Reigber et al. 1983). The elaboration of the most recent fourth's generation model series, GRIM4, being accomplished during the last years, was motivated

Correspondence to: F. Barlier

by new satellite missions requiring most precise orbit restitution: on the French side the SPOT-2 mission with its first employment of the French DORIS Doppler tracking system (launched in 1990), and the American/French altimeter mission TOPEX/POSEIDON with its laser, DORIS and GPS tracking systems (launched in 1992); on the German side the European ERS-1 and ERS-2 altimeter missions (launched in 1991 and 1995) supported by laser tracking and the German PRARE microwave tracking system; PRARE unfortunately did not succeed on ERS-1 due to a failure in the space segment but works nominally on ERS-2 and METEOR-3. With respect to these missions the French group "Groupe de Recherche de Géodésie Spatiale" (GRGS) of the French Space Agency CNES in Toulouse is responsible for the qualification of the DORIS Doppler tracking system whereas the German group with GeoForschungsZentrum Potsdam (GFZ) is charged with the operational ERS-1/-2 orbit determination and altimeter data reduction within the framework of ESA's German Archiving and Processing Facility for ERS-1/-2 (D-PAF) located at the German Aerospace Research Centre (DLR) in Oberpfaffenhofen near Munich.

The most recent GRIM4 global gravity field models are called GRIM4-S4 and GRIM4-C4. The S4-model is a satellite-only solution deduced through orbit perturbation analysis technique from optical, laser, and microwave tracking data of 34 satellites including also ERS-1 laser and TOPEX/POSEIDON GPS satellite-to-satellite tracking as well as ERS-1 and TOPEX/POSEIDON altimeter cross-over differences. The C4-model combines the satellite-only normal equation system with surface gravity data, i.e. $1^\circ \times 1^\circ$ mean gravity anomalies over the continents plus recently released data over Russia, South America, Asia, and Greenland, and GEOSAT, ERS-1, and TOPEX/POSEIDON altimeter data over the oceans through a computed mean sea surface reduced by the Levitus dynamic sea surface topography. The combination model represents a homogeneous spectral resolution of the Earth's gravity field complete up to degree and order 72 in terms of spherical harmonics, a truncature equivalent to a minimum wavelength of 555 km at the Earth's surface. Due to the attenuation of the gravity signal with altitude, the resolution of the satellite-only model can be considered to be complete only up to about degree and order 30 with higher frequency information within some distinct orders. Satellite-only solutions underlie altimeter derived quasi-stationary sea surface topography models and are applied in precise orbit determination of altimeter satellites to prevent aliasing with implicit sea surface modelling.

The harmonic coefficients for the gravitational geopotential are simultaneously solved for in a least squares adjustment together with ocean tidal terms for 8 partial waves, tracking station positions for over 300 optical, laser and Doppler stations and tracking station velocities for 14 well occupied laser stations.

Compared to the first GRIM4 model pair, GRIM4-S1/C1 (Schwintzer et al. 1991), a considerable improvement has been achieved through the inclusion of more and new satellite tracking data, in particular DORIS Doppler, GPS satellite-to-satellite tracking data and altimeter cross-over differences, and through the availability of new surface gravity data. The GRIM4 state-of-art global gravity field models compare with the JGM models jointly worked out at the American Centre for Space Research of the University of Texas in Austin and the NASA Goddard Space Flight Center in Washington.

2. Computational Model Description

2.1. Mathematical Representation

The GRIM4 static gravitational model expresses the Stoke's normalised coefficients $(\overline{C}_{lm}, \overline{S}_{lm})$ of a spherical harmonic expansion of the Earth's gravitational potential U complete from degree 0 up to maximum degree $l_{max} (= 72$ for GRIM4-C4), except the terms $\overline{C}_{10}$, $\overline{C}_{11}$, $\overline{S}_{11}$, $\overline{C}_{21}$, $\overline{S}_{11}$ which are fixed to zero in order to identify the model's origin with the Earth's centre of mass and its reference axis with the Earth's inertial axis. Therefore:

$$\begin{aligned} U(r,\phi,\lambda) &= \sum_{l=o}^{l_{\max}} \sum_{m=o}^{l} U_{lm} \\ &= \frac{GM}{r}\left[\overline{C}_{oo} + \sum_{l=2}^{l_{\max}} \sum_{m=o}^{l} \left(\frac{R}{r}\right)^l \overline{P}_{lm}(\sin\phi) \right. \\ &\qquad \left. (\overline{C}_{lm}\cos m\lambda + \overline{S}_{lm}\sin m\lambda)\right] \end{aligned} \tag{1}$$

with
l, m: degree, order
r, ϕ, λ: spherical coordinates of a point (radius, latitude, longitude)
R: reference length ($\approx$ semi-major axis of a reference ellipsoid)
$\overline{P}_{lm}$: normalised Legendre polynomials $(m = 0)$ and associated functions $(m > 0)$
GM: product of the gravitational constant by the mass of the Earth.

The Earth's gravitational potential U is going to be recovered by (a) the satellite orbit perturbation technique and (b) surface data evaluation : the GRIM4-S4 model is deduced from satellite tracking data only whereas in the GRIM 4-C4 model surface data complete the information derived from satellite orbit perturbation analyses. Surface data are issued either from gravimetric measurements and processed in the form of mean free air gravity anomalies per degree square

$$\Delta g(\phi,\lambda) = \frac{1}{r(\phi)} \sum_l (l-1)\left(U_{lo} - U_{lo}^* + \sum_{m\neq o} U_{lm}\right) \tag{2}$$

or from altimetric measurements under the form of geoid heights per degree square

$$N(\phi,\lambda) = \frac{1}{\gamma(\phi)} \sum_l \left(U_{lo} - U_{lo}^* + \sum_{m\neq o} U_{lm}\right) \tag{3}$$

with:
U^*_{lo}: normal gravitational potential term of degree l of the chosen conventional reference ellipsoid (only depending of even degree zonal coefficients: $\overline{C}^*_{2n,o}$).
$r(\phi)$: radius at latitude ϕ on the ellipsoid
$\gamma(\phi)$: normal gravity at latitude ϕ on the ellipsoid

The time varying part of the GRIM4 gravity model contains a secular drift of the flattening term $\overline{C}_{20}$ (in parts per year) and 76 sensitive low degree and order terms (degree 2 to 6, order 1 to 3) of the spherical harmonic expansion of the ocean tide potential for 8 diurnal or semidiurnal waves: Q_1, O_1, P_1, K_1, N_2, M_2, S_2, K_2. The total potential issued from the usual spherical harmonic expansion of the ocean tide heights describes the attraction of a variable single layer of water on the Earth surface

$$\Delta U = 4\pi GR\rho_w \sum_n \sum_{l,m} \sum_{+}^{-} \frac{1+k'_l}{2l+1} \left(\frac{R}{r}\right)^{l+1} C^{\pm}_{n,lm} \sin\left(\theta_n \pm m\lambda + \varepsilon^{\pm}_{n,lm}\right) P_{lm}(\sin\phi) \quad (4)$$

with
n: wave-number
l, m: degree, order
$+/-$: prograde/retrograde terms
G: gravitational constant (6.672 10^{-11} m^3 kg^{-1} s^{-2})
ρ_w: mean water density (1025 kg m^{-3})
θ_n: Doodson argument of the wave n
k'_l: loading Love number per degree
$C^{\pm}_{n,lm}$: amplitude of the tidal constituent
$\varepsilon^{\pm}_{n,m}$: phase relative to Greenwich meridian

2.2. Initial and Underlying Models and Constants

The models and constants adopted for the gravity field modelling computations are summarised in Table 1. To a large extent the IERS Standards (McCarthy 1992) or the Project MERIT Standards (Melbourne et al. 1983) have been followed.

2.2.1. Reference Coordinate Systems

The underlying Earth-fixed Conventional Terrestrial System (CTS) is defined by its origin, the geocentre and the orientation of the X-axis at epoch 1984.0, which is close to the Greenwich meridian. The Y-axis is pointing to the East. The orientation of the Z-axis of the CTS is defined by the mean pole position over the time interval 1/1980 through 10/1986 (zero mean pole) and is $\Delta\overline{x}_p = .045''$ and $\Delta\overline{y}_p = .286''$ apart from the CIO-pole. As a consequence the offsets $\Delta\overline{x}_p$, $\Delta\overline{y}_p$ are subtracted from the smoothed homogeneous 1962–1987 pole series ERP(BIH)87C02 (Feissel and Guinot 1988) and from 1988 onward from the values as published in the yearly or monthly IERS Bulletin reports.

These series of 5-day or 1-day pole positions (x_p, y_p) were used for the rotation of the mean terrestrial system into the "true" terrestrial system. The third component of the Earth rotation parameters series, Θ (true Greenwich sidereal time), is applied for rotating the system into the "true" equatorial system in which the satellite's equations of motion are integrated. These Earth

Table 1a. Summary of GRIM4 Computational Model

REFERENCE SYSTEM		
CIS		mean equator and equinox of J2000.0[1)]
Precession		IAU 1976[1)]
Nutation		IAU 1980[1)] + Herring 1987 correction/IERS correction
Earth rotation		x_p, y_p, Θ: ERP(BIH)87C02[1)], IERS Bulletin B[1)] (x_p, y_p transformed to zero mean pole)
CTS:		
Z-axis		ERP(DGFII)87L03 : zero mean pole 1/1980 – 10/1986
X-axis		SSC(DGFII)87L03 (epoch 1984.0)
time evolution		no-global-net-rotation[1)]
Origin		Earth's centre of mass[1)]
Velocity of light (scale)		c = 299792458 m/s[1)]
DYNAMICAL MODEL		
Earth		R = 6378136m[1)]
		1/f = 298.25781 (inverse flattening of reference ellipsoid)
		ω = 0.7292115.10^{-4} rad s^{-1} (mean angular velocity of Earth)
	*	GM = 398600.440 km^3/s^{21}, C_{00} = 1[1)]
	*	GRIM3-MX or GRIM4-C2 gravity models (epoch 1984.0), C_{21}, S_{21} modelled with respect to zero mean pole (effect of pole tide not considered) solid tides[1)] (Wahr (2,2). k_2 = 0.3, δ = 0, permanent tide not removed)
	*	ocean tides (GRGS (19, 4) spher. harm. model from Schwiderski[1)] 1° × 1° grid, 11 tides, Sa = 0)
Third bodies		Sun and 5 planets as point masses, Moon with Ferrari 1977 (4,4) gravity model, DE200/LE200 ephemerides[1)]
Relativity		none
Surface forces :		
along-track acceleration	*	empirical (LAGEOS, NOVA-1, -3, ETALON)
1/rev acceleration	*	empirical (GEOSAT, ERS1)
atmospheric drag	*	DTM (Barlier et al. 1978)
solar radiation	*	solar constant 4.5605.10^{-6} Nm^{-2} at 1 AU[1)], exponential regularising function
Earth radiation		albedo and infrared (Stephens et al. 1981)
area/mass ratio		satellite dependent (variable for TOPEX/POSEIDON, ERS-1)

Table 1b. Summary of GRIM4 Computational Model

GEOMETRICAL MODEL		
Station positions	*	laser (after 1979): SSG (DGFII) 87L03, -89L03
(epoch 1984.0)	*	Doppler: GRGS solution (transformed)
	*	optical, laser (up to 1979): GRIM3-L1 (transformed)
Station horizontal velocities	*	SSC (DGFII) 87L03, AMO-2 (Minster and Jordan 1983), NUVEL-1 (De Mets et al. 1990)
Site displacements:		
Earth tides		Wahr[1)]
Ocean loading		based on Schwiderski ocean tide model
Pole tide		IERS 1989[1)]
Tropospheric refraction		laser: Marini and Murray (1973)[1)]
Ionospheric refraction		Doppler: first order correction obtained from the difference of two frequency measurements
Frequency offset/drift	*	Doppler: pass-by-pass correction (OSCAR-19: arc-by-arc drift)
Relativity		range and Doppler effect[2)]
Parallactic refraction		optical: see Veis (1960), p. 119
Annual aberration		optical: see Haefner, Martin (1966) (aberration constant equal to 20.49552'')

* - initial values/models foreseen partly/entirely for adjustment
1) - values/models according to IERS Standards (McCarthy 1992)
2) - values/models according to MERIT Standards (Melbourne 1983)

rotation parameters were kept fixed to their initial values in the present GRIM4 solutions although in principle they can be estimated from the data. The rotations due to precession, and nutation connect the ''true'' equatorial system to the (quasi) space-fixed Conventional Inertial System (CIS) at epoch J2000.0.

The reason for adopting the zero mean pole instead of the CIO-pole is to keep the $\overline{C}_{2,1}$, $\overline{S}_{2,1}$ coefficients of the gravity model, which are a function of the actual and mean pole position and $\overline{C}_{2,0}$ (Reigber 1981), close to zero. However this is quite equivalent to keeping the IERS reference frame and adopting the following $\overline{C}_{21}, \overline{S}_{21}$ values: $\overline{C}_{21} = -1830\ 10^{-9}, \overline{S}_{21} = 1.1628\ 10^{-9}$.

The origin of the system coincides with the Earth's centre of mass which is the focal point of any adjusted satellite's orbit, being also connected to the adjusted tracking station positions via the observation equations. Within this geocentric system the first degree terms of the spherical harmonic expansion of the geopotential are forced to be zero ($\overline{C}_{10} = \overline{C}_{11} = \overline{S}_{11} = 0$) because these coefficients are proportional to the coordinates of the centre of mass with respect to the origin of the coordinate system (Heiskanen and Moritz 1967).

2.2.2. Dynamic Models and Constants

The Dynamic Model characteristics are given in Table 1a which summarises all model parameters and constants which enter in the description of forces acting on a satellite. Those terms marked with an asterisk are foreseen to be partly or entirely adjusted. In this case the given values or models are the initial ones to be corrected by the adjustment.

The initial gravity model is based on a GRIM3 solution (Reigber et al. 1985). Most of the satellite data were processed using this a priori field, except SPOT-2, TOPEX, ERS-1, STELLA, METEOR-3 and LAGEOS-2 which were processed based upon the more recent model GRIM4-C2, to ensure a better linearization. In order to combine properly all normal equations, the right-hand sides have to be transformed to account for the difference between both sets of a priori values.

The Schwiderski tidal model (Schwiderski 1980) was chosen as the initial one, taking into account the amplitudes and phases of 11 partial tides. The spherical harmonic decomposition of the model was computed with a maximum degree $l = 19$ and a maximum order $m = 4$. A total of 76 selected terms out of these constituents are adjusted in the GRIM4 solutions, covering all 8 non-zonal tidal waves in the Schwiderski representation.

2.2.3. Geometric Model

The Geometric Model characteristics referring to tracking station initial positions, and observation related models, quantities and corrections are given in Table 1b.

The initial geocentric station positions were taken from a coordinate solution based on a LAGEOS laser data evaluation (Reigber et al. 1988). For all stations, horizontal movements due to plate tectonics are modelled. The rates of change in position are taken, if available, from the initial LAGEOS solution, or from the geophysically derived AMO-2 (Minster and Jordan 1983) or NUVEL-1 (DeMets et al. 1990) plate motion models. The horizontal velocities were adjusted in the GRIM4 solutions for a selected set of 14 laser stations with accurate and dense observations over a sufficiently long period of time.

2.3. Data Base and Data Processing

2.3.1. Satellite Tracking Data

Gravity field recovery from satellite tracking data employs the satellite trajectory perturbation technique. Observables of type range (Laser), biased range (GPS-

SST), range rate (Doppler), direction (camera), and/or radial cross-over difference are used to restitute the orbit of a satellite. The numerically integrated orbit, by a Cowell algorithm, over a few days (typically 3 days to 30 days) is adjusted to the observations by an iterative least squares process. The partial derivatives with respect to the arc initial orbital elements, drag and radiation pressure scale factors, gravity field parameters, ocean tides parameters, station coordinates, and nuisance parameters are computed for each single measurement within one orbital arc. The least squares process adopted for minimising the residuals between the observed minus computed quantities eventually generates the normal equation system for each arc. The systems for different arcs are then accumulated according to a chosen initial and relative weighting scheme depending on the satellite and type of data, then the resulting system is solved by inversion after having introduced additional constraints and stabilizing equations.

The optical data collected from the early sixties through the early seventies have an accuracy of about 2", for a near-Earth satellite with an altitude of about 1000 km this corresponds to a pointing accuracy of about 10 m or to a relative accuracy of

$$\sigma_{opt} = 1 \cdot 10^{-5} \hat{=} 2''/1 \text{ rad.}$$

Satellite laser ranging started systematically in 1967 with the DIADEME campaign, but more extensively in 1971 with the ISAGEX campaign, where the tracking accuracy was about 1 to 5 m depending on the stations. Since then the accuracy has improved to about 50 cm for the second generation lasers up to the late seventies and to better than 5 cm for the third generation laser tracking network operating since 1980. In summary, the orbit of a 1000 km high flying typical satellite was, in this analysis, considered to be observed by satellite laser ranging with relative accuracies of:

$$\sigma_{las} = 5 \cdot 10^{-6} \hat{=} 5 \text{ m}/1000 \text{ km for the 1967 and 1971 campaigns}$$
$$5 \cdot 10^{-7} \hat{=} .5 \text{ m}/1000 \text{ km after 1975}$$
$$\text{and} \quad 5 \cdot 10^{-8} \hat{=} .05 \text{ m}/1000 \text{ km after 1980.}$$

Relative accuracies within the 10^{-8} level (or even better) are also obtained with GPS satellite-to-satellite biased ranging and satellite altimetry.

Doppler tracking data have been acquired since the early sixties. They were assigned a typical accuracy of a few mm/s (TRANET Doppler). With DORIS on board SPOT-2 and TOPEX/POSEIDON, this accuracy is around .3 mm/s. At the altitude of 1000 km with the satellite velocity being about 7 km/s, we get the following relative accuracy figures:

$$\sigma_{dop} = 2 \cdot 10^{-7} \hat{=} 1.5 \text{ mm}/7 \text{ km (TRANET Doppler)}$$
$$\sigma_{dop} = 4 \cdot 10^{-8} \hat{=} .3 \text{ mm}/7 \text{ km (DORIS Doppler)}$$

There is a total of 34 satellites in our solution as can be seen from Table 2, where the complete statistics on the satellite tracking data exploited in the GRIM4-S4 solution is given. The orbit altitudes of the satellites used range from about 800 km to 20000 km. It follows that 15 of the 34 satellites are tracked by cameras, 17 by laser and 9 by microwave (Doppler, GPS) instrumentation, some of these with mixed optical/laser or laser/microwave systems at the same time.

Although the optical and old laser data are comparatively poor in accuracy and volume it has been decided to use them because only with the inclusion of these satellites can a good distribution in inclination be achieved, especially with regard to the inclinations below 50°.

TOPEX and ERS-1 have been treated with particular care. Not only the laser and DORIS tracking measurements on TOPEX/POSEIDON and the laser measurements on ERS-1 have been used in GRIM4, but also the mixed altimeter crossover points between TOPEX/POSEIDON and ERS-1 (plus TOPEX/POSEIDON and ERS-1 single satellite crossovers) as additional tracking observations. ERS-1, at a much lower altitude than TOPEX/POSEIDON, experiences more drag and the laser data solely do not allow to solve for many empirical drag parameters. Introducing a relative radial constraint w.r.t. the TOPEX/POSEIDON orbit through the mixed crossovers helps to better separate gravity field and drag coefficients (one coefficient every 6 hours and 1/rev empirical acceleration) at ERS-1 altitude. On the whole, one 35 day orbit repeat cycle of ERS-1 in 1993 corresponding to three and a half cycles of TOPEX/POSEIDON was processed simultaneously for a mixed altimeter cross-over point generation.

2.3.2. Earth Surface Data

The GRIM4-C4 in addition to the S4 model incorporates $1° \times 1°$ mean values of free air gravity anomalies (mainly over the continents), and marine geoid heights issued from altimetry. Thanks to this contribution the combined model results in a complete solution up to degree/order 72 without the necessity to introduce any constraint for stabilising the normal matrix as compared to the satellite-only solution.

The mean gravity anomaly data set was established by combining different data sets over Greenland (Forsberg, Private Communication), China (Lithospheric Dynamics Atlas of China, State Seismological Bureau, 1989), Former Soviet Union (Makedonskii et al. 1994), South America (SAGP Project, GETECH 1991), with the OSU90 data set (Rapp et al. 1991). This compilation contains $1° \times 1°$ mean free air anomalies derived from measured point values over land or sea or predicted by topoisostatic models (parts of Africa). The gravity anomalies were corrected to account for the mass of the atmosphere by adding a mean value of .87 mgal.

Marine geoid data are directly issued from the $1° \times 1°$ GRGS GEOSAT/ERS-1/TOPEX mean sea surface (GRGS Computation, Cazenave et al. 1995). From the sea surface heights the Levitus dynamic topography (Levitus 1982) was subtracted to get geoid

Table 2. Characteristics of satellite orbits and tracking data included in the GRIM4 models

Satellite Name	*I*	*a*	*Ecc.*	Resonance period	No. of Arcs × length		Number of Observations			Observ. period
	(*)	(km)		(d)	(weeks)	Opt.	Laser	μ-wave	Acti/Xover	(Y–1900)
PEOLE	15.0	7006.	.016	2.1	5	78	588	–	–	71
COURIER-1B	28.3	7469.	.016	3.8	11	2844	–	–	–	66–67
VANGUARD-2	32.9	8298.	.164	2.7	10	2082	–	–	–	66
EXPLORER-9	38.8	7960.	.108	9.0	10	3568	–	–	–	62
D1-D	39.5	7622.	.085	8.4	11	5832	1983	–	–	67/71
D1-C	40.0	7341.	.053	2.5	13	2364	3773	–	–	67/71
BEACON-C	41.2	7507.	.026	5.6	20	–	35999	–	–	79/83
TELSTAR-1	44.8	9669.	.243	14.9	12 × 2	3828	–	–	–	62–64
ECHO-1RB	47.2	7966.	.012	11.9	6 × 3	1804	–	–	–	65
STARLETTE	49.8	7331.	.020	2.8	122	–	58521	–	–	83–84, 86–88
AJISAI	50.0	7869.	.001	3.6	70	–	42716	–	–	86–88
ANNA-1B	50.1	7501.	.008	4.8	16	3194	–	–	–	66
LAGEOS 2	52.0	12278	.078	2.8	8 × 4	–	30908	–	–	92–93
GEOS-1	59.4	8075.	.072	7.0	39	–	41910	–	–	77–78
ETALON-1	65.0	26400.	.001	7.9	16 × 4	–	5032	–	–	89/90
ETALON-2	65.0	26400.	.001	7.9	3 × 4	–	1975	–	–	90
TOPEX	66.0	7714.	.001	3.3	7	–	7213	143585	–	92
					6	–	10417	178615	8278	93
TOPEX/GPS					1 × 1d	–	–	2 × 5955	–	92
					5 × 2d	–	–	2 × 73983	–	93
GEOS-3	114.9	7226.	.001	4.5	25	–	17698	–	–	75–77
GEOS-3/ATS-6					–	–	–	36730	–	75–78
TRANSIT-4A	66.8	7300.	.008	3.5	8	512	–	–	–	62
AGENA	69.9	7295.	.001	5.0	3 × 2	472	–	–	–	64
LAGEOS-1	109.8	12273.	.004	2.7	52 × 4	–	292414	–	–	83–87
GEOSAT	108.0	7163.	.001	2.9	20 × .5	–	–	443426	–	86/87
					3	–	–	37336	–	86
GEOS-2	105.8	7711.	.033	5.7	54	–	37265	–		75–77
EXPLORER-19	78.7	7800.	.100	2.0	27	3280	–	–		65
BEACON-B	79.7	7354.	.014	3.0	21	1542	1157	–		64–71
STELLA	98.7	7178	.001	4.0	15	–	4280	–	–	93
ERS-1	98.5	7153.	.001	3.0	21	–	16468	–	–	92
					7	–	3684	–	5360	93
ERS-1/TOPEX					6	–	2462	–	12032	93
SPOT-2	98.2	7210.	.001	6.2	23 × .5	–	–	249392	–	91
METEOR-3	82.6	7573	.002	10.0	12	–	20335	–	–	94
MIDAS-4	95.8	9995.	.011	3.0	48 × 2	46814	–	–	–	64–65
OGO-2	87.4	7341.	.075	3.6	11	774	–	–	–	66
OSCAR-19	90.2	7460.	.018	2.5	18	–	–	125241	–	84
NOVA-1	90.0	7557.	.001	5.5	16	–	–	123596	–	84
NOVA-3	90.0	7571.	.003	6.2	55	–	–	439266	–	87
n_{sat} = 34					836	78988	636808	1937063	25670	

heights. Data blocks over shallow water (depth < 200 m) were eliminated.

3. Solution Strategies

Each individual normal equation system resulting from the satellite tracking data processing as described in the previous section is reduced by the arc-dependent parameters: satellite position and velocity at the beginning of each arc, two to 30 surface force and empirical acceleration parameters, pass dependent frequency offset and drift in the case of Doppler observations and ambiguities and clock parameters for GPS carrier phase and pseudorange observations. Then the reduced systems, containing only the common parameters, are accumulated and eventually augmented by external information to yield a full rank normal equation system. Below are outlined the procedures applied for the generation of the satellite-only solution, i.e. based upon satellite tracking data only, as well as for the generation of the combined solution, i.e. incorporating in addition Earth's surface observation data such as gravity anomalies from land and sea gravimetry and sea surface heights from altimetry.

3.1 Satellite-only Solution

Earth's orbiting satellites basically sense linear combinations of coefficients belonging to certain orders of the gravitational spectrum. The most pronounced orbit

perturbations arise from the zonal coefficients ($m = 0$) and from the tesseral/sectorial coefficients around the resonant orders $m = 12$ to 14, $m = 27$ to 29, and $m = 41$ to 44. This is valid for satellites flying at altitudes ranging from 800 km to 1200 km, as it is the case for most of the satellites used here (Kaula 1966, Reigber 1989). The contribution of one individual coefficient within a resonant order mainly depends on the orbit inclination (Klokoćnik 1985). Therefore a large variation in the inclinations of the satellite orbits involved is important for a good algebraic separation of the solve-for coefficients in the adjustment. With increasing altitude the gravitational signal in the satellite orbit gets attenuated due to the factor $(R/r)^l$ in Equation (1) ; also resonances occur in other orders than quoted above. With the satellite tracking data actually available a homogeneous coverage with respect to resolution and accuracy of all spectral parts of the gravitational potential complete to a truncation degree and order of e.g. 60 cannot be achieved.

This results in all ill-conditioned normal equation system after having accumulated all individual satellite normal equation systems, which requires to apply some regularizing procedure before inversion. This procedure on the one hand has to resolve (near-) linear relations within the normal equations and on the other hand has to add strength to those coefficients lacking enough information. We adopted the method by which stochastic a priori information is introduced as a direct observation equation for each unknown gravitational coefficient $\overline{C}_{lm}$ and $\overline{S}_{lm}$, respectively:

$$\{\overline{C}_{lm}, \overline{S}_{lm}\} = 0 \pm \sigma_l \tag{6}$$

σ_l : formal standard deviation derived from the coefficients' degree variance law according to Kaula's rule of thumb, $\sigma_l \approx 10^{-5}/l^2$.

The weighting of the observation equations (6), which are written for all solve-for coefficients with a degree larger than $l = 5$, is c/σ_l^2 with c being a relative weight factor (see below). Kaula's rule of thumb reflects the decrease in magnitude of the coefficients with increasing degree, as derived from an early analysis of terrestrial gravity data (Kaula 1966). The normal equation system resulting from equations (6) has a diagonal structure.

Other external normal equation systems are created for station position unknowns from survey ties connecting different occupations at the same tracking site. In the same way the optical and Doppler station networks also are related to the most precise laser stations.

To overcome the rank deficiency in the normal equation system which appears when solving for all tracking station positions, geodetic datum constraints have to be introduced to define the origin, scale and orientation of the coordinate system if not sensed by the data themselves. Six of the seven possible degrees of freedom of a cartesian geocentric coordinate system (X, Y, Z) are already implicitly modelled: the scale through the use of laser distance measurements (velocity of light), the origin as the geocenter, which is the focal point of all Earth orbiting satellities, and the orientation of the Z-axis by fixing the given pole coordinates and their evolution with time. There is one degree of freedom left, i.e. the orientation of the X and Y-axis in the equatorial plane (rotation about the Z-axis), with respect to which the initial set of station coordinates can be defined through the following condition equations (Bender and Goad 1979):

$$\sum_i \cos^2 \phi_i^o (\lambda_i - \lambda_i^o) = 0 \tag{7}$$

$$\sum_i \cos^2 \phi_i^o (\dot{\lambda}_i - \dot{\lambda}_i^o) = 0 \tag{8}$$

with
λ_i^o, ϕ_i^o: initial values of longitude and latitude of i-th station
λ_i: a posteriori longitude of i-th station
$\dot{\lambda}_i^o, \dot{\lambda}_i$: initial and a posteriori value, respectively, of the rate of change in longitude of i-th station.

Equation (8) prevents a common rotation about the Z-axis when adjusting the horizontal rates of change in position of the tracking stations (due to plate tectonics). The early satellite camera observations contain information about the absolute orientation of the reference frame via their connection to the star coordinates, but the accuracy is by more than one order too low and insufficient to provide the reference for the precise laser observations. Therefore 14 LAGEOS laser stations, each one with a multi-year tracking record, are selected to enter into the geodetic datum condition equations (7, 8). These are then treated like two highly weighted observation equations to form an additional external normal equation system.

After having created all individual data and external information equation systems the following processing steps are run through:

- accumulation of reduced normal systems for each satellite,
- summing up the satellite-wise accumulated normal equation systems and the system containing the stochastic a priori information, thereby applying empirically additional relative weighting, and subsequently adding the normal equation systems from survey ties and datum fixation,
- solution of the resulting (total) normal equation system by Cholesky matrix inversion,
- evaluation of the solution by error propagation and intercomparisons with external models and data sets.

The last three steps are repeated, each time applying a different weighting scheme, until an optimum result is achieved.

Table 3 lists the initial and eventually found relative weights assigned to the different data sets.

Compared to the initial "realistic" weighting the 11 optical satellites had to be upweighted because, due to their sometimes unique orbits with low inclinations and high eccentricities, they considerably contribute to the

Table 3. GRIM4-S4/C4 satellite tracking data weighting scheme

Data set	Std. dev.σ	weight
camera	2"–4"	10 σ^{-2}
old laser (before 83)	100–300 cm	10 σ^{-2}
mixed camera/laser		0.1 σ^{-2}
ATS-6/GEOS-3 SST	0.2 mgal	0.1 σ^{-2}
laser:		
LAGEOS-1/2	6–20 cm	0.1 σ^{-2}
ETALON-1/2, ERS-1, TOPEX, STELLA, METEOR-3	6–20 cm	1 σ^{-2}
STARLETTE, AJISAI	25–30 cm	1 σ^{-2}
Doppler:		
OSCAR-19	5–12.5 mm/s	1 σ^{-2}
GEOSAT	3–12 mm/s	1 σ^{-2}
NOVA-1/-3	3 mm/s	1 σ^{-2}
SPOT-2 (DORIS)	2 mm/s	0.25 σ^{-2}
TOPEX (DORIS)	0.7 mm/s	1 σ^{-2}
GPS-SST:		
TOPEX	4 cm (phase), 100 cm (pseudorange)	1 σ^{-2}
altimeter crossovers:		
ERS-1	12.5 cm	1 σ^{-2}
TOPEX/POSEIDON	20 cm	1 σ^{-2}
mixed ERS-1/ TOPEX/POSEIDON	20 cm	1 σ^{-2}
stochastic a priori information (Kaula), only in GRIM4-S4	$\sigma_1 = 10^{-5}/l^2$	100 σ_1^{-2}

overall strength of the resulting normal equation system. The very precisely and intensively observed satellites like LAGEOS and SPOT-2 had to be downweighted in order to get a balanced solution. Moreover it was necessary to overweight the stochastic a priori information by a factor of c = 100 (found empirically) in order to get a stable solution.

For each observation equation (6) the partial redundancy

$$f_i = 1 - q_{ii}(c/\sigma_l^2) \tag{9}$$

can easily be computed a posteriori with the diagonal terms q_{ii} of the cofactor matrix Q_p of the adjusted gravitational unknowns $x_i = \{\overline{C}_{lm}, \overline{S}_{lm}\}$. The partial redundancy with $0 \le f_i \le 1$ is a measure for the degree of contribution of the stochastic a priori information to the determination of the associated solve-for parameter x_i with respect to the contribution coming from the real observation data:

When $f_i = 0$ then x_i is estimated to 100% from stochastic a priori information and to 0% from real observations, when $f_i = 1$, then x_i is estimated to 0% from stochastic a priori information and to 100% from real satellite tracking observations.

In case of $f_i = 0$ the associated unknown can be deleted from the system and in case of $f_i = 1$ the additional stochastic a priori observation equation can be omitted without changing the adjustment results. The lower the value f_i the more the associated gravity coefficient is constrained to zero according to equation (6) (Schwintzer 1990).

The final normal equation system contains the following unknowns to be determined explicitly:

- gravitational geopotential (stationary part): 3758 spherical harmonic coefficients $\overline{C}_{lm}$, $\overline{S}_{lm}$, complete to degree/order 60 including C_{oo}, plus higher degree and order terms within ERS-1 and SPOT-2 resonant orders (m = 13 and 57) up to a maximum degree of 69 (as mentioned in Chapter 2.2.1, the degree one terms are fixed to zero and the coefficients $\overline{C}_{21}, \overline{S}_{21}$ are not adjusted but modelled as described in Reigber, 1981)
- secular variation of the dynamic Earth's flattening $\overline{C}_{20}$
- ocean tide potential: 76 ocean tide constituents (unknown parameters are amplitude and phase angles) for 8 diurnal and semidiurnal partial waves up to maximum degree 6
- station coordinates (epoch values): geocentric Cartesian coordinates X, Y, Z for 323 tracking stations
- horizontal station velocities: rates of change in latitude and longitude for 14 selected LAGEOS laser stations with sufficiently long observation periods; the motions of all other tracking stations are modelled according to the AMO-2 (Minster and Jordan 1983) or the more recent NUVEL-1-NNR (De Mets et al. 1990) geophysical plate motion model.

3.2. Combined Solution

For combining the satellite-only normal equation system with the Earth's surface data, normal equations from the following gridded data sets (mean $1^\circ \times 1^\circ$ values) were created applying empirically found optimal weights according to the standard deviations given below:

– OSU90 + BGI provided "observed" free-air gravity anomalies over land: $\sigma_i = 3.2$ mgal,
– OSU90 "observed" free-air gravity anomalies over sea, if not covered by altimetry: σ_i = 3.2 mgal
– OSU90 predicted free-air gravity anomalies over land and sea, if not covered by altimetry: $\sigma_i = 6.4$ mgal
– GEOSAT/TOPEX/ERS-1 altimeter derived ocean geoid (Levitus sea surface topography subtracted from mean sea surface heights): $\sigma_i = 32$ cm.
– GRIM4-S4 derived gravity anomalies filling remaining gaps for a complete global data coverage: $\sigma_i = 6.4$ mgal.

Gap filling and avoidance of multiple coverage of identical blocks proved to be necessary for obtaining a stable solution. The final weight p_i was assigned to each block value according to the formula:

$$p_i = (\sigma_0^2 \,/\, \sigma_i^2)\cos^2\phi\ , \quad \sigma_0^2 = 1 \tag{10}$$

The weighting takes into account the decreasing area of the equiangular blocks with increasing latitude $|\phi|$.

Table 4 lists the number of originally given and eventually used surface data points.

The normal equations systems, as defined above, are accumulated and combined with the GRIM4-S4 normal equation system, this time excluding the stochastic a

Table 4. Number of considered surface data

Source	Gravimetry $1° \times 1°$ Δg	Sea Grav. $1° \times 1°$ Δg	Predicted $1° \times 1°$ Δg	Altimetry $1° \times 1°$ N	Gaps $1° \times 1°$ Δg	Sum
Available data:						
OSU90/BGI	13 130	31 996	5 667	–	–	50 793
GRGS (GEOSAT/ERS-1/TOPEX)	–	–	–	33 539	–	33 539
Used data:						
OSU90/BGI	12 206	4 696	5 625	–	–	22 527
GRGS(GEOSAT/ERS-1/TOPEX)	–	–	–	28 258	–	28 258
GRIM4-S4	–	–	–	–	14 015	14 015
						64 800

Δg - gravity anomalies, N - geoid heights

priori information which now is replaced by the surface data.

When combining the normal equation systems from satellite tracking data and surface data the gravitational coefficients up to degree/order 5 are kept separated and different coefficients are implicitly determined for the gravity anomalies and ocean geoid data sets. These precautions are applied to avoid a degradation of the solution arising from long-wavelength errors and residual (sometimes unknown) reference system discrepancies in the surface data. The gravitational coefficients up to degree and order 5 associated with the surface data are treated like nuisance parameters and reduced beforehand. The vectors of unknowns enlarges to 5252 gravitational coefficients (stationary part) according to the complete set up to degree and order 72.

4. Results

Two solutions both including gravitational harmonic coefficients, ocean tide constituents and tracking station position parameters, were obtained as usual with the former GRIM4 models: a satellite only solution, GRIM4-S4, giving gravitational coefficients up to degree 60 plus a few zonal terms and resonance terms up to degree 69 and a combined solution with gravity anomaly and altimeter data, GRIM4-C4, developed up to degree and order 72. The solved-for tidal and position parameters are identical for both solutions.

The reason for providing a satellite-only model (GRIM4-S4) along with the combined model (GRIM4-C4) is the independence of the satellite-only solution from any assumptions concerning the sea surface topography. By this, the geoid derived from the satellite-only gravity field model can be employed as the underlying reference surface for modelling the very long-wavelength quasi-stationary sea surface topography from sea surface heights measured by altimetry (it should be noted however that an accurate restitution of the gravity field by satellite means is limited to the very low degrees of the field namely up to degrees 10 to 15). Even if the sea surface topography is solved simultaneously with the gravitational geopotential from the altimeter data in a combined gravity field solution, assumption are to be made concerning the shorter wavelength spectral part of the sea surface topography and the variability over the data evaluation period, thus affecting the geoid solution. In the GRIM4-C4 solution the sea surface topography is estimated up to degree and order 5, i.e. the very long-wavelength spectral part revealing the signatures larger than about 8000 km and representing a temporal average over a 10 years period. The higher frequency spectral part of the sea surface topography has been modelled according to the Levitus climatologic model (Levitus 1982).

Both models, GRIM4-S4 and GRIM4-C4, are equally well efficient for satellite orbit computations (orbit altitudes exceeding about 800 km), whereas the geoid, due to the lack in power from degree 15 upwards in the GRIM4-S4 model, is more completely represented by the combined solution GRIM4-C4: spatial resolution of geoidal features about 2000 km with GRIM4-S4 vs. 500 km with GRIM4-C4 (full wavelength). The higher degree terms ($1 > 36$), hardly sensed by the satellites used, decrease considerably in power in the satellite-only solution and converge to zero due to the stochastic a-priori- information introduced (cf. Equation 6).

Fig. 1 shows the partial redundancies f_i computed from Equation (9) for each stochastic a priori information Equation (6) related to any particular geopotential coefficient $\overline{C}_{lm}$. As the pattern looks quite similar for the $\overline{S}_{lm}$ coefficients, the second figure is suppressed. Following the discussion in Chapter 3.1 and remembering that a large value f_i, which always varies between 0 and 1, indicates a weak, and a small value f_i a strong contribution of the stochastic a priori information to the estimated coefficient value, then the black and dark grey shaded coefficients in Fig. 1 are estimated with an amount of information coming from the satellite tracking data to at least 50%, whereas the light grey shaded coefficients are determined to more than 50% by the stochastic a priori information (i.e. Kaula's degree variance with best fitting relative weight). Those coefficients, for which $f_i = 0$, lack of any satellite tracking data contribution and therefore are constrained to zero in the adjustment according to Equation (6).

It can be deduced from Fig. 1 that there is a distinct sensitivity of the totality of the used tracking data to the zonal geopotential coefficients up to degree 45, to the non-resonant and weak resonant coefficients (order 1 through 11, 16 through 23) up to about degree 30,

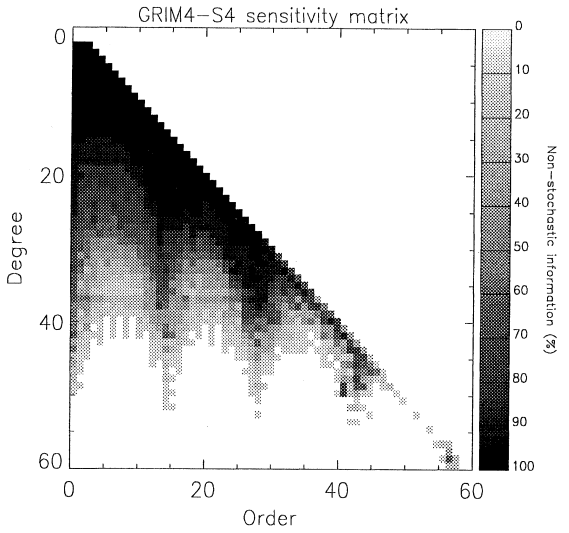

Fig. 1. GRIM4-S4 sensitivity matrix. Partial redundancies of stochastic a priori information equations

increasing up to degree 45 for the strong first resonant and second resonant terms around orders 14 and 28, respectively. There exists also a distinct sensitivity within the third resonant and even for the fourth resonant terms (around orders 42 and 58, resp.).

Fig. 2 depicts signal and error degree curves (scaled according to Chapter 5.1) in terms of geoid heights (m). The geographic distribution of the GRIM4-C4 geoid errors is drawn in Fig. 3 as derived by rigorous error propagation (using the full covariance matrix).

The C4 model is not completely free from any kind of constraint: the distribution of altimetric and gravimetric data displays two major gaps at the poles, beyond the polar circles. In order to reduce distortions of the geoid due to a weakness in the normal equation system, we were obliged to add fictitious gravity data in these areas issued from the S4 model, so that the Earth is completely covered by one degree square surface information. The fact that the S4 model is very smooth at high degrees and truncated at degree 60 generates a small loss of power in the C4 model, particularly manifest between degrees 61 and 72 as revealed in Fig. 2. This procedure generates larger errors in the high latitude zones because of the lower weight of the fictitious data as can be seen on the geoid height error map (Fig. 3) computed from the GRIM4-C4 variance-covariance matrix.

Table 5 lists the a posteriori obtained basic model parameters ; $\overline{C}_{oo}$, inferred GM, $\overline{C}_{20}$ at epoch 1984.0, the drift of $\overline{C}_{20}$ and the low degree Stokes coefficients (up to degree and order 10) together with their standard deviations calibrated as explained in Chapter 5.1.

Table 6 gives the adjusted values in amplitude and phase of the parameters of the 8 ocean waves of the GRIM4-C4 solution (no significant difference to GRIM4-S4 solution) compared to the original Schwiderski values and to a more recent hydrodynamic model, (IMG-FES95.2 model, Le Provost et al. 1994). Long period waves (S_a, S_{sa}, M_m, M_f) which are not very sensitive in terms of orbital disturbances were kept fixed at the Schwiderski's values. It has to be mentioned that the 18.6 year wave was not modelled. The standard deviation given for the adjusted parameters are a posteriori scaled by a factor of $c = 5$ (cf. Chapter 5.1).

Seasonal variations in the low degree gravitational harmonics are not considered in the present solutions and the absence of the 18.6 year equilibrium tide surely affects the adjusted value of the secular variation in $\overline{C}_{20}$.

Geocentric coordinates of all 323 tracking stations involved were adjusted realising a homogeneous reference frame. In addition, horizontal station velocities of 14 well tracked laser stations have been determined. However, due to not solving for Earth rotation parameters and to the limited data periods (e.g. for

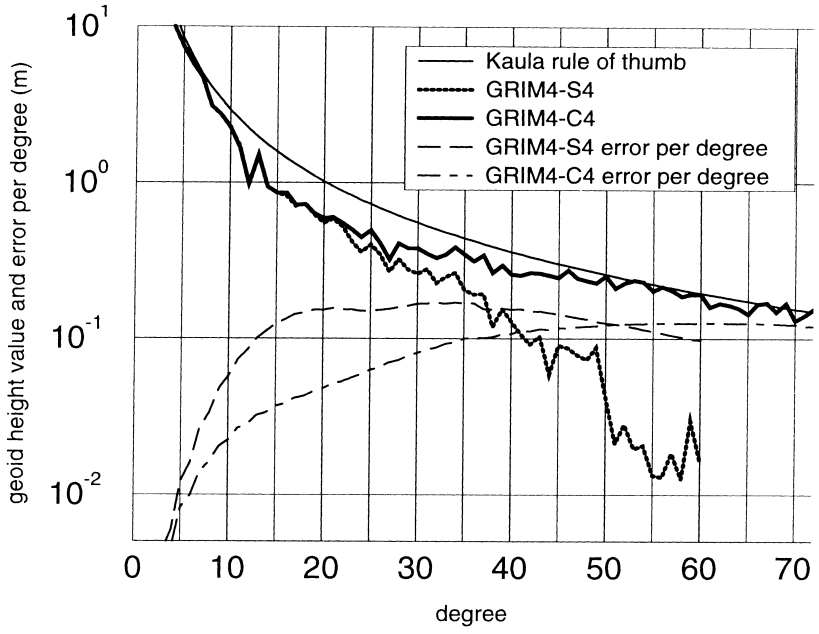

Fig. 2. Signal/error per degree for GRIM4-S4/C4 in terms of geoid height

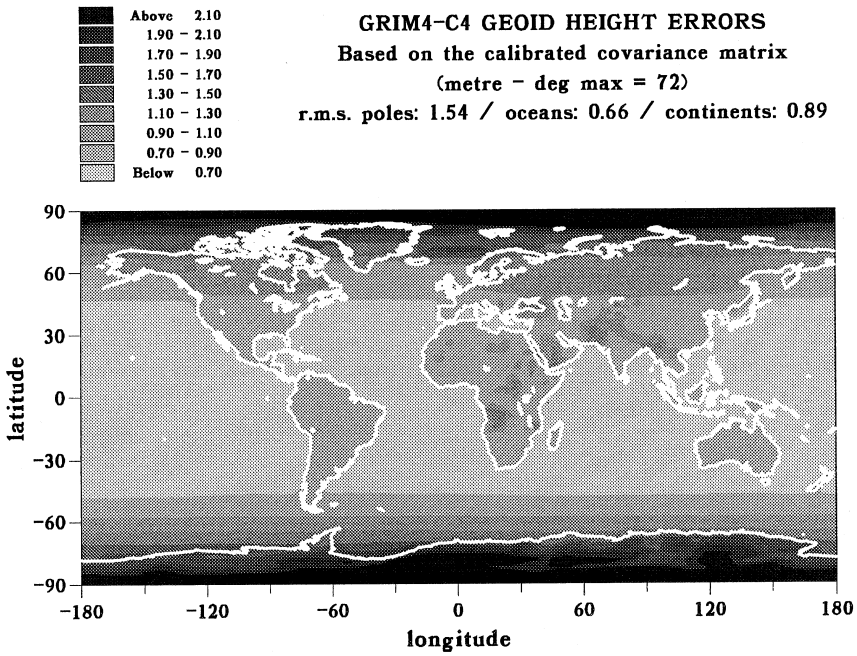

Fig. 3. GRIM4-C4 geoid height errors

LAGEOS) exploited in the GRIM solution, the accuracy and reliability of the horizontal station motions obtained are inferior to those of a dedicated LAGEOS or GPS/IGS solution. The horizontal velocities of the 14 basic stations (no significant differences to GRIM4-S4 solution) are compared in Table 7 with the values from the NUVEL-1NNR geophysical model (De Mets et al. 1994). The standard deviations given for the adjusted velocity components are posteriori scaled by a factor $c = 5$ (cf. Chapter 5.1).

5. Evaluation of the GRIM4-S4 and C4 solutions

The accuracy of the gravity field solutions is evaluated by intercomparisons with external data sets and precise satellite orbit computations with tracking and altimeter data using the gravity field model under investigation. The intercomparisons in terms of geoid heights, gravity anomalies, and altimeter cross-over differences resulting from the precise orbit computations are used to calibrate the variance-covariance matrix of the adjusted parameters by a single factor, in order to transform the formal errors into more realistic ones. The formal errors in terms of standard deviations of the adjusted parameters are due to aliasing of modelling errors and shortcomings in the stochastic model by far too optimistic. The calibrated variance-covariance matrix can then be used to represent the internal quality of the gravity field model, for instance to study geographically the precision of the geoid.

Taking into account noise, truncation errors (due to a lack of spectral power in a satellite-only model) and non-gravitational errors in the data sets used for comparisons and cross-over computations, a factor of $c^2 = 25$ was adopted to scale the variance-covariance matrix, i.e. the formal standard deviations are increased by a factor $c = 5$ in order to get a realistic estimate of the GRIM4-S4 commission errors (c.f. Table 8). The same calibration factor was applied to the GRIM4-C4 variance-covariance matrix, as this model is based on the GRIM4-S4 normal equation system.

5.1. Calibration

Although the use of a single calibration factor for scaling the error variances of the whole variety of unknowns is quite questionable as well as the lax procedure to derive this factor, it wasn't considered worth developing a more sophisticated method.

Rigorous error propagations were performed starting with the unscaled variance-covariance matrix of the adjusted spherical harmonic coefficients of the GRIM4-S4/C4 models to predict average standard deviations in terms of geoid undulations, gravity anomalies and cross-over differences (Rosborough 1987, Balmino 1992). These values are compared to the rms values of geoid and gravity anomaly differences from independent external comparisons and computed ERS-1 cross-over differences, cf. Table 8.

5.2. Internal evaluation of GRIM4-S4/C4

Fig. 4 and 5 show the geoid standard deviations of the GRIM4-C4 and S4 models for each pair of coefficients (C_{lm}, S_{lm}). For the S4 model it clearly appears that, besides the very long wavelength parts, only zonal terms and a narrow sectorial band with a few resonance terms are well determined (standard deviations below 1 cm). The slowly increasing precision from degree 40 clearly shows the increasing influence of the a priori constraint given by Kaula's rule. Such a model is in fact able to

Table 5. GRIM4-S4/C4 normalised coefficients (*1.10^9) up to degree and order 10, 1) inferred GM (km^3/s^{-2}), 2) (drift/year)*10^9, 3) excluding permanent tide

deg.	ord.	GRIM4-S4				GRIM4-C4			
l	m	$\bar{C}_{lm}$	σ	$\bar{S}_{lm}$	σ	$\bar{C}_{lm}$	σ	$\bar{S}_{lm}$	σ
0	0	−5.8	.6			−5.5	.6		
		398600.4377	.0002	1)		398600.4377	.0002	1)	
2	0	.029	.004	2)		.024	.004	2)	
2	0	−484165.6	.1	3)		−484165.6	.1	3)	
3	0	957.3	10.3			957.3	10.3		
4	0	540.4	.3			540.2	.2		
5	0	68.6	.1			68.7	.1		
6	0	−150.9	.7			−150.6	.4		
7	0	90.9	.4			90.6	.2		
8	0	50.9	1.3			50.5	.6		
9	0	27.2	1.0			28.2	.4		
10	0	51.2	2.1			51.7	.8		
3	1	2030.4	.3	248.3	.3	2030.1	.3	248.4	.3
4	1	−535.2	.2	−473.2	.2	−535.3	.2	−473.5	.2
5	1	−62.7	.8	−93.9	.8	−61.7	.6	−94.6	.6
6	1	−78.0	.8	25.5	.7	−77.2	.5	26.4	.5
7	1	280.6	1.6	93.0	1.5	278.2	.8	95.0	.8
8	1	27.0	1.6	59.9	1.6	25.2	.8	58.4	.8
9	1	141.1	2.6	26.1	2.4	144.9	1.0	21.9	1.0
10	1	79.2	2.6	−131.5	2.6	82.3	1.0	−130.4	1.0
2	2	2439.3	.1	−1400.0	.1	2439.3	.1	−1400.0	.1
3	2	905.1	.3	−619.1	.3	905.0	.2	−619.4	.2
4	2	350.4	.5	662.8	.5	350.9	.3	662.6	.3
5	2	651.0	.8	−323.7	.8	651.3	.5	−322.6	.5
6	2	48.8	1.1	−373.6	1.1	48.3	.7	−373.0	.7
7	2	332.2	1.6	93.4	1.7	331.7	.9	92.0	.9
8	2	79.2	2.0	64.2	2.0	79.6	.9	63.7	.9
9	2	17.9	2.5	−31.5	2.6	19.2	1.1	−31.2	1.1
10	2	−93.2	3.0	−47.3	3.0	−93.1	1.0	−48.2	1.1
3	3	721.3	.2	1414.3	.2	721.3	.1	1414.3	.1
4	3	990.8	.2	−201.0	.2	991.0	.2	−201.1	.2
5	3	−451.2	.5	−215.7	.5	−451.1	.3	−215.8	.3
6	3	58.7	.8	8.7	.8	58.2	.5	9.0	.5
7	3	248.9	1.3	−214.9	1.4	249.2	.7	−215.5	.7
8	3	−20.3	1.8	−85.2	1.7	−18.9	.9	−86.0	.9
9	3	−157.5	2.4	−79.3	2.6	−158.3	1.0	−78.1	1.0
10	3	−5.9	2.9	−156.4	2.8	−6.8	1.1	−155.5	1.1
4	4	−188.4	.1	−308.7	.1	−188.3	.1	308.8	.1
5	4	−295.0	.3	49.6	.3	−295.1	.2	49.4	.2
6	4	−86.0	.5	−471.6	.5	−85.8	.3	−471.7	.3
7	4	−275.4	.8	−124.6	.8	−275.1	.5	−123.4	.5
8	4	−244.8	1.3	70.1	1.3	−245.0	.6	70.8	.6
9	4	−8.2	1.9	22.8	1.9	−9.2	.8	19.3	.8
10	4	−84.1	2.4	78.2	2.5	−83.9	1.0	−80.5	1.0
5	5	174.7	.2	−669.0	.2	174.8	.2	−669.0	.2
6	5	−267.0	.2	−536.7	.2	−266.9	.2	−536.6	.2
7	5	3.0	.5	18.5	.5	2.5	.3	18.4	.3
8	5	−25.1	.7	89.9	.8	−25.3	.4	89.4	.4
9	5	−19.6	1.3	−55.1	1.3	−17.9	.7	−53.9	.7
10	5	−51.4	1.8	−52.7	1.9	−49.7	.7	−51.4	.7
6	6	9.3	.1	−237.7	.1	9.3	.1	−237.7	.1
7	6	−358.8	.2	151.8	.2	−358.7	.2	151.8	.2
8	6	−66.2	.3	308.5	.3	−65.9	.2	308.8	.2
9	6	63.5	.7	222.7	.7	63.5	.4	222.6	.4
10	6	−37.1	1.0	−79.3	1.0	−38.2	.5	−80.0	.5
7	7	1.9	.2	24.1	.2	2.0	.2	24.1	.2
8	7	67.4	.2	75.1	.2	67.3	.2	75.0	.2
9	7	−117.5	.4	−96.4	.4	−117.9	.3	−96.7	.3
10	7	8.0	.5	−3.9	.5	8.2	.4	−3.4	.4
8	8	−123.9	.2	120.8	.2	−124.0	.2	120.7	.2
9	8	188.1	.3	−3.1	.3	188.3	.2	−2.8	.2
10	8	40.9	.3	−91.7	.3	40.9	.3	−91.4	.3
9	9	−47.7	.2	96.3	.2	−47.7	.2	96.3	.2
10	9	125.6	.2	−38.0	.2	125.4	.2	−38.1	.2
10	10	100.5	.2	−23.7	.2	100.4	.2	−23.7	.2

Table 6. Ocean tides parameters adjusted in the GRIM4-C4 solution and comparison with the Schwiderski and IMG-GES95.2 models

Doodson Number	Darwin Symbol	deg	ord	GRIM4-C4				Discrepancies to Schwiderski (1980)		IMG-FES95.2 (1995)	
		l	m	C^+_{lm} (cm)	σ	ε^+_{lm}(°)	σ	ΔC^+_{lm}	$\Delta^{\varepsilon+}_{lm}$	ΔC^+_{lm}	$\Delta^{\varepsilon+}_{lm}$
135.655	Q1	2	1	.89	.10	310.1	6.5	−.35	3.6	−.34	4.6
135.655	Q1	3	1	.44	.13	125.9	16.2	−.13	−18.4	−.10	−22.7
135.655	Q1	4	1	.05	.16	99.9	164.3	.24	189.0	.24	187.9
135.655	Q1	5	1	.37	.14	104.2	22.3	−.15	8.2	−.15	8.8
145.555	O1	2	1	2.89	.09	313.3	1.7	−.47	.4	−.28	−.3
145.555	O1	3	1	1.51	.11	72.4	4.1	−.19	11.1	−.08	10.0
145.555	O1	4	1	1.82	.14	270.4	4.2	−.39	5.9	−.18	7.7
145.555	O1	5	1	1.04	.14	107.3	7.1	−.10	1.8	.07	3.4
163.555	P1	2	1	1.20	.07	318.6	3.4	−.30	−4.6	−.20	−3.7
163.555	P1	3	1	.49	.08	55.1	9.2	−.19	−15.2	−.11	−15.6
163.555	P1	4	1	.70	.13	262.7	10.8	−.07	−4.4	.01	−5.7
163.555	P1	5	1	.40	.16	125.1	20.3	.01	−20.6	.06	−19.9
165.555	K1	2	1	2.88	.07	327.3	1.4	−.07	−12.1	.12	−11.6
165.555	K1	3	1	1.09	.08	40.4	4.0	−.20	−6.6	−.03	−5.8
165.555	K1	4	1	2.11	.14	246.9	3.7	−.20	7.3	.02	8.6
165.555	K1	5	1	1.43	.16	82.0	5.3	−.22	22.6	−.07	22.2
245.655	N2	2	2	.67	.04	340.2	3.1	−.01	−18.5	.02	−8.5
245.655	N2	3	2	.08	.03	176.5	23.3	.02	−4.4	.00	−1.1
245.655	N2	4	2	.34	.04	132.5	6.2	−.12	9.3	−.10	10.9
245.655	N2	5	2	.06	.02	90.5	20.2	.02	−85.5	.01	−86.0
245.655	N2	6	2	.07	.04	348.8	29.8	.00	−2.0	−.00	12.2
255.555	M2	2	2	3.25	.03	322.1	.5	−.29	−11.5	−.04	−.6
255.555	M2	3	2	.32	.03	178.9	5.4	.04	−9.8	−.02	−4.0
255.555	M2	4	2	1.02	.03	129.7	1.9	−.02	−4.8	.04	.3
255.555	M2	5	2	.33	.02	13.7	3.4	−.05	−17.0	−.04	−6.2
255.555	M2	6	2	.38	.03	329.4	4.6	.03	−.2	.03	2.2
255.555	M2	3	3	.51	.04	34.6	4.9	−.02	−1.3	−.06	−.2
255.555	M2	4	3	.20	.01	183.2	3.7	.03	−.0	.02	−4.8
273.555	S2	2	2	.82	.03	301.4	1.8	−.20	−.6	.03	5.0
273.555	S2	3	2	.19	.02	192.1	8.0	.08	10.0	.12	14.1
273.555	S2	4	2	.43	.03	113.7	3.6	−.05	−10.6	−.05	−6.8
273.555	S2	5	2	.27	.02	115.9	4.5	−.13	−112.1	−.11	−93.6
273.555	S2	6	2	.12	.03	243.9	15.2	.05	36.6	.06	43.2
275.555	K2	2	2	.34	.03	319.5	4.4	−.08	−4.4	−.05	−.5
275.555	K2	3	2	.13	.03	149.7	9.7	−.03	45.5	−.05	55.3
275.555	K2	4	2	.09	.03	104.0	15.7	.02	−.4	.00	−.8
275.555	K2	5	2	.21	.02	34.9	6.1	−.17	−34.3	−.18	−7.2
275.555	K2	6	2	.10	.00	272.8	1.8	−0.6	8.5	−.05	19.8

Table 7. Horizontal station velocities in mm/year from the GRIM4-C4 solution

number	Station site	GRIM4-C4 north	σ	east	σ	NUVEL1-NNR north	east
7086	McDonald	−1.7	6.1	−20.0	7.2	−7.1	−12.0
7090	Yaragadee	86.7	3.5	19.9	2.3	59.2	38.9
7105	Greenbelt	13.9	3.1	−28.1	2.9	3.6	−15.0
7109	Quincy	−2.9	3.5	−30.6	2.6	−13.2	−12.8
7110	Monument Peak	8.0	3.1	−49.6	2.4	22.4	−40.9
7122	Mazatlan	−.4	10.0	−20.6	8.8	−8.1	−9.4
7210	Heleakala	26.4	3.7	−68.7	2.2	32.2	−58.3
7834	Wettzell	18.0	5.0	23.8	5.1	13.5	20.3
7835	Grasse	11.8	2.5	15.3	2.5	14.4	20.0
7838	Simosato	−5.2	4.5	−6.1	4.0	10.1	−10.2
7839	Graz	18.8	2.7	8.3	2.6	13.0	21.1
7840	Herstmonceux	10.3	2.2	4.0	2.7	15.2	17.7
7907	Arequipa	18.6	5.1	.7	4.7	9.4	−3.3
7939	Matera	19.7	5.0	13.6	4.5	12.8	22.0

Table 8. GRIM4-S4 propagated standard deviations vs. observed differences

GRIM4-S4	geoid mean 5° × 5° block values	gravity	ERS-1 cross-over differences
Formal error:			
rms (std.dev.) before scaling	15 cm (I_{max} = 36)	0.6 mgal (I_{max} = 36)	1.7 cm (I_{max} = 60)
Observed:			
rms (differences) w.r.t altimetry	80 cm (I_{max} = 36)	4.4 mgal (I_{max} = 36)	13.5 cm (I_{max} = 60)
Commission error:			
rms (std. dev.) after scaling (scaling factor: c = 5)	75 cm (I_{max} = 36)	3.0 mgal (I_{max} = 36)	8.5 cm (I_{max} = 60)

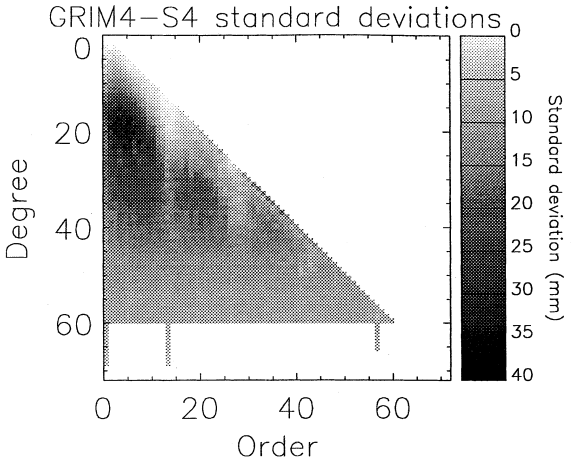

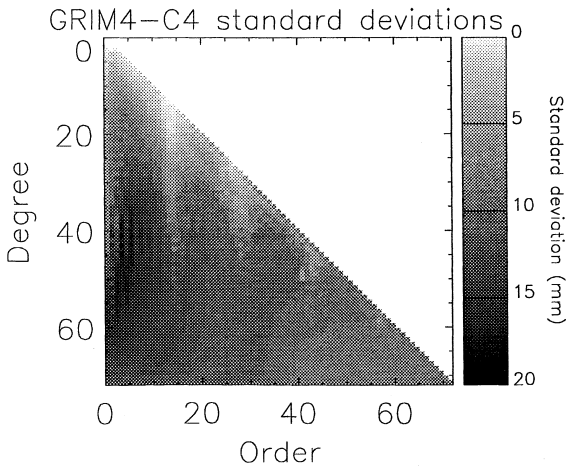

Fig. 4–5. GRIM4-S4C4 standard deviations in terms of geoid heights (scaled by factor 5)

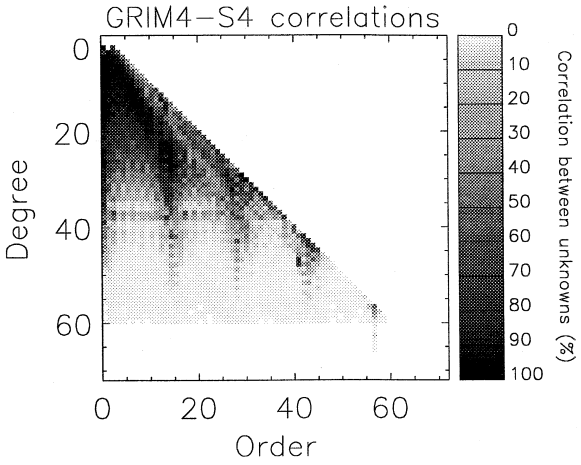

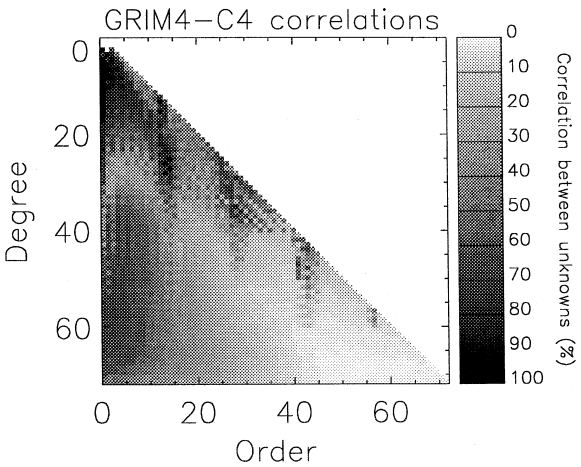

Fig. 6–7. GRIM4-S4C4 correlations between unknowns in percent

give only a good long-wavelength geoid (e.g. up to degree 15) and it is performing well for orbit computations of satellites with altitudes above about 800 km.

The pattern of the standard deviations per degree and order of the C4 model is quite similar for low degrees but completely different for high degrees. The fact that it is similar at low degrees means that there is little impact of altimetry and gravimetry data at these degrees. There is anyway almost no impact for degrees 0 to 5, the coefficients for these degrees having been determined separately for each set of surface data entering the C4 model. At higher degrees, resonances excepted, one can see a propagation of increasing errors towards low orders. This is probably due to the lack of surface information at the poles which generates more instability at high degrees and low orders.

But it is not satisfactory to analyze only the variances of parameters which have a non-diagonal variance-covariance matrix. Covariances contain important information on the algebraic separability of individual parameters to be solved. Fig. 6 and 7 reveal that the low degree coefficients (except the sectorial band) are the most correlated ones and those within some satellite resonance orders such as 12 to 15 and 25 to 29.

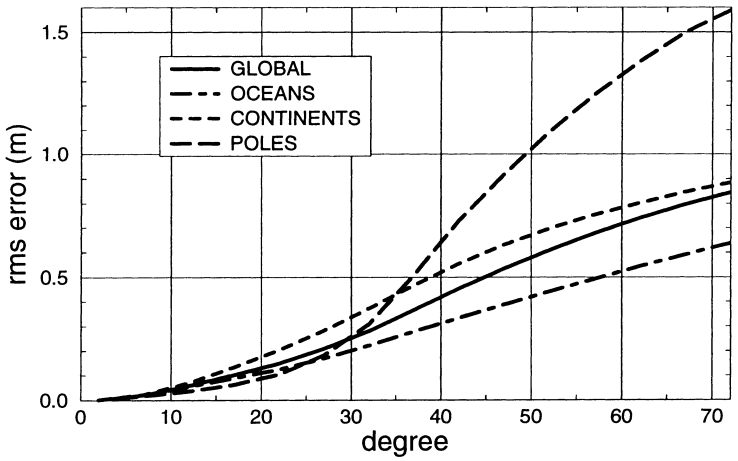

Fig. 8. GRIM4-C4 Cumulated geoid error

This is due to the impact of satellite tracking data which principally produces correlations between even and odd degree coefficients, respectively, within a particular order, as satellites mainly see linear combinations of these coefficients.

It is then of great importance to make use of the full variance-covariance matrix in order to get a realistic idea of the precision of the solution. This was effectively done for recovering the geoid error, the radial mean orbit error at different inclinations, and the radial mean orbit error mapped over the Earth's surface for a given satellite.

The geoid error (Fig. 8) based on the GRIM4-C4 calibrated variance-covariance matrix confirms the fact that we have a poor knowledge over the polar caps due to lack of data: the error reaches close to the poles one to two meters. A clear difference also appears between continents and oceans due to the types of surface data and the different weighting which had to be taken into account. One globally gets a precision of 89 cm r.m.s. on continents and of 64 cm on the oceans (Fig. 8), when taking into account the commission error up to degree/order 72 (down to the 555 km wavelenth). The geoid comparison with JGM3 (Tapley et al. 1994) (Fig. 9) presents a similar pattern by zone and a good agreement for the global feature.

The calibrated variance-covariance matrix has also been used to predict radial orbit errors at the altitude of ERS-1, i.e. 777 km and TOPEX, i.e. 1336 km. On Fig. 10 and 11 this error is plotted for orbit inclinations between 30° and 150°. The symmetric pattern relative to the polar inclination is typical for present geopotential models and results from the spatial distribution of the satellite orbits being exploited in the solution. So the minima, at the cm level for the STARLETTE, SPOT, TOPEX, ERS-1 inclinations for example are well marked; besides, the increasing errors at low inclinations come from the absence of well tracked low inclined geodetic satellites.

A more complex information is given, for instance for the ERS-1 orbit, by the map of the predicted geographically correlated radial orbit errors (Fig. 12). These results reflect the part of the orbit signal which may go into the recovered sea surface heights from ERS-1 altimetric measurements: it reaches globally 3.3 cm rms. For TOPEX the error decreases to about 1.4 cm rms.

Fig. 13 and 14 show how the GRIM4-C4 model matches with the terrestrial data used. One can see that the assimilation of the data into the model is not completely achieved. Even filtered at degree 72, the gravimetric data compare at the level of 7.7 mgal rms and discrepancies greater than 10 or 20 mgals appear

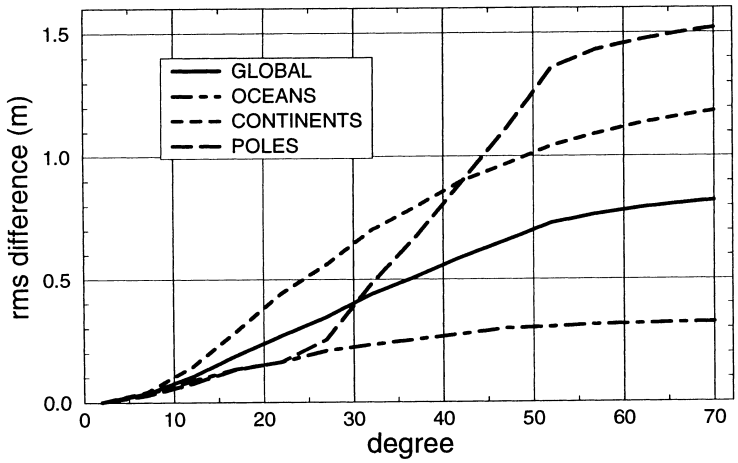

Fig. 9. GRIM4-C4/JGM3 Cumulated geoid difference

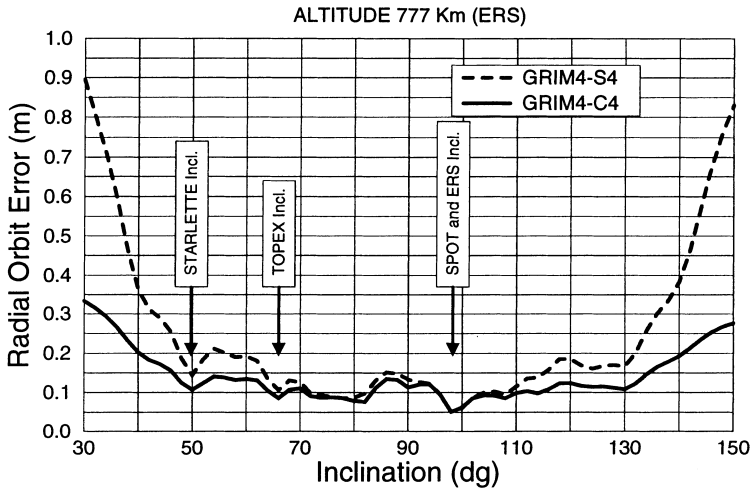

Fig. 10. Radial orbit error as a function of inclination

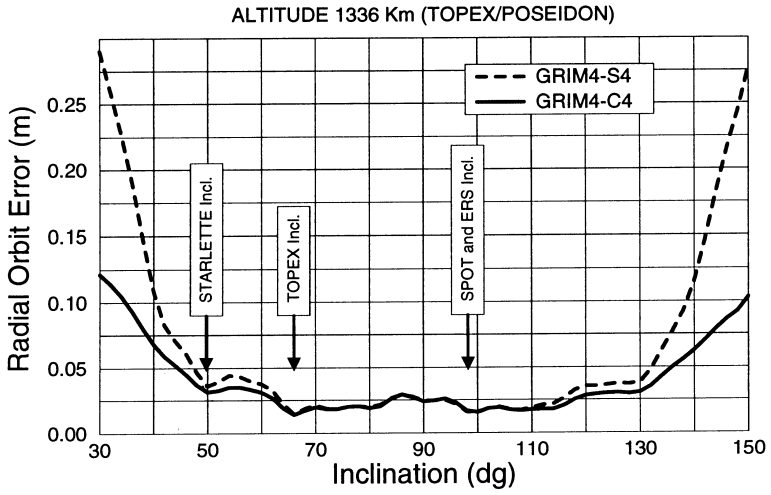

Fig. 11. Radial orbit error as a function of inclination

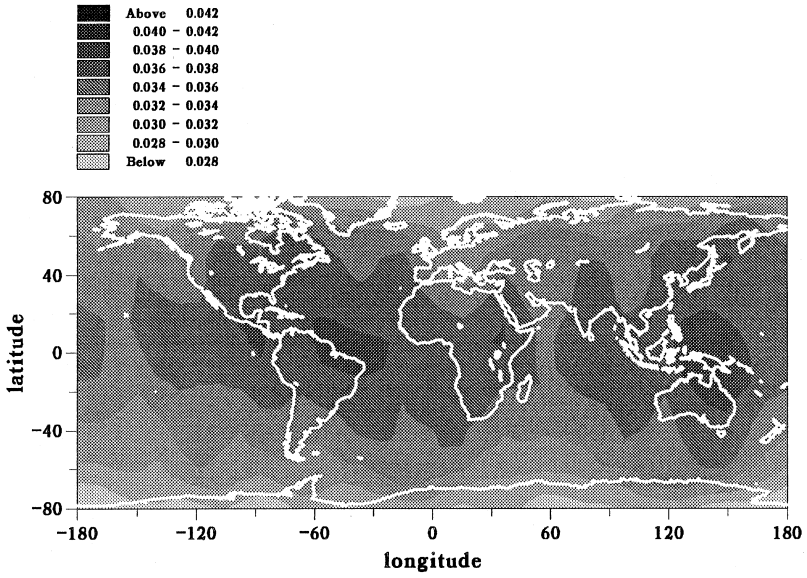

Fig. 12. Radial orbit error (mean part) for the ERS-1 and 2 orbit based on the calibrated covariance matrix (meters)

e.g. over the Andes, some parts of Africa and Himalaya. The marine geoid data used are issued from a GEOSAT/TOPEX/ERS-1 mean sea surface. There remains a 36 cm rms difference with the C4 model, reaching 1 to 2 meters or even more in high latitudes. Inhomogeneities hence appear between the different types of data used in

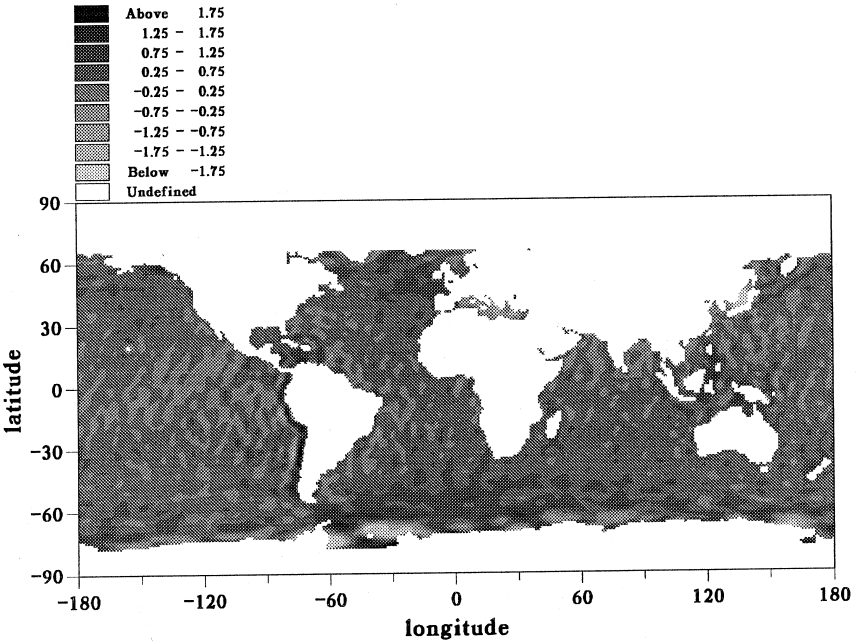

Fig. 13. Geoid height differences : GRIM4-C4 minus Filtered Altimetric Data (meters - deg max = 72) r.m.s. = 0.36 m / max = 4.8 m

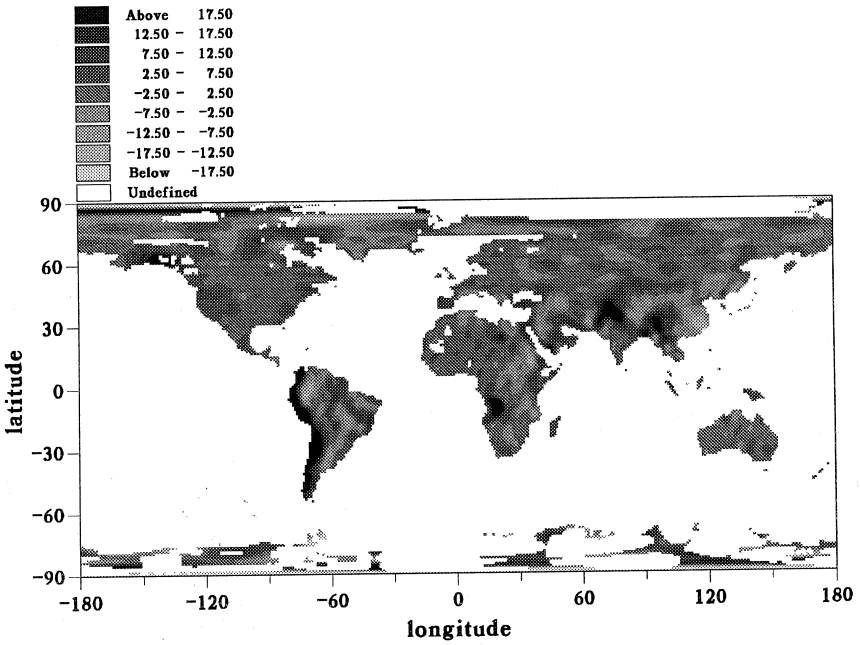

Fig. 14. Gravity anomalies differences: GRIM4-C4 minus filtered gravimetric data (mgal – deg max = 72) r.m.s. = 7.7 mgal / max = 85 mgal

the GRIM4-C4 solution and it is not excluded that problems may exist on some sets of terrestrial data over particular areas.

5.3. Comparison with External Data Sets

Point or equal angular mean block values of geoid undulations and gravity anomalies, have been computed from the spherical harmonic coefficients of the GRIM4-S4 and the GRIM4-C4 model, respectively. These values have been differenced with various data sets:

- 1°× 1°, geoid from two years of ERS-1 altimetry, denoted MSS93 (Gruber et al., 1993).
- 5°× 5° geoid from ERS-1 (35d, 168d orbit cycles)/ TOPEX altimetry, denoted MSS95a (Anzenhofer et al. 1995).
- 5°× 5° geoid from GEOS-3/SEASAT/GEOSAT altimetry, denoted OSU92 (Basic and Rapp 1992).
- 5°× 5° geoid from ERS-1/TOPEX/GEOSAT altimetry denoted OSU95 (Rapp 1995).
- 5°× 5° gravity anomalies from SEASAT altimetry, denoted Marsh89 as provided by J. Marsh, NASA/ Goddard Space Flight Center, in 1989.
- 5°× 5° gravity anomalies from terrestrial free-air anomalies, denoted OSU89 (Kim and Rapp 1990); only values between latitudes ± 75 ° were considered.
- set of globally distributed point geoid undulations (1261 values), denoted DGL90, compiled from

various sources and derived from Doppler or GPS measured ellipsoidal heights minus orthometric heights observed by terrestrial levelling.
– 5°× 5° geoid and 5°× 5° gravity anomalies computed from the JGM2S (Nerem et al. 1994) satellite-only and the JGM3 (Tapley et al. 1994) combined global gravity field models, respectively.

From the overall differences computed for an individual data set, the weighted root mean sum of squares (wrms) of the residuals has been calculated after adjusting a constant bias to account for differences in the underlying reference systems. A weight proportional to the cosines of latitude was adopted. In the case of the DGL90 data set a statistical outlier procedure is applied, rejecting all data points with a residual larger than twice its standard deviation.

Table 9 gives the results of the comparisons for the GRIM4-S4 and C4 solutions, also for the American global gravity field models JGM2-S and JGM3. Whereas the satellite-only models are independent of the altimetry/gravimetry data sets used for intercomparisons, this is of course not true for the combined solutions.

The better fit of the combined solutions GRIM4-C4 and JGM3 to the surface data compared to the satellite-only solutions is due to the increased signal power when incorporating altimeter and surface gravity data. The fit to a 1°× 1° geoid and to point undulations is worse than the fit to a 5°× 5° geoid due to the truncation error inherent in a long-wavelength gravity field model. The altimetry data sets covering ocean areas are more homogeneous and accurate than the OSU89 data set derived from terrestrial gravimetry which reveals therefore larger discrepancies.

It can be deduced from Table 9 that, at least over the oceans, state-of-the-art global satellite-only gravity field models represent the long-wavelength part of the geoid ($\lambda/2 > 550$ km) equally well to an accuracy of about 75 cm and gravity to about 4 mgal, and state-of-the-art combined global gravity field models, taking into account all gravity information presently available, achieve the 25 cm and 3 mgal levels, respectively. The fact that the JGM3/GRIM4-C4 geoid discrepancies (wrms = 0.43 m) exceed this level indicates a poorer performance in high latitude areas not covered by altimetry.

5.4. Orbital tests

Orbital fit to tracking data constitutes a good quality test of the models and allows to compare the performances of the GRIM4 models with respect to other current gravity field models.

A set of laser, DORIS-Doppler, GPS-Satellite-to-Satellite-Tracking and altimetric cross-over measurements on seven satellites has been chosen to evaluate the capability of the GRIM4 models in orbit computation. The other models considered for comparison are the satellite-only model JGM2S (Nerem et al. 1994) - to be compared to GRIM4-S4- and the combined model JGM3 (Tapley et al. 1994). The rms of fit to the tracking data shown in Table 10 is derived from 5 arcs chosen during the period 1993–1995 for each satellite.

Except for the GPS-SST data, any of the tracking data used in this set did not directly contribute to the GRIM4 models. For each arc the following dynamic model parameters were estimated:

Table 9. Intercomparisons with external data sets, wrms (min... max) of residuals after bias adjustment (N-geoid undulation, Δg-gravity anomaly, n: number of non-rejected points, *comparison up to degree 50 only)

Data Set	Data Type (Unit)	Resolution	GRIM4-S4 JGM2-S	GRIM4-C4 JGM3
Altimetry				
MSS93	N (m)	1° × 1°	1.41 (−17.1...10.1)	0.77 (−9.7...8.6)
			1.39 (−14.9...9.9)	0.76 (−9.9...8.7)
MSS95a	N (m)	5° × 5°	0.76 (−4.4...3.2)	0.30 (−2.9...1.2)
			0.73 (-5.7...2.7)	0.24 (−3.0...1.2)
OSU92	N (m)	5° × 5°	0.75 (−4.5...2.8)	0.25 (−3.0...1.6)
			0.72 (−3.8...2.5)	0.21 (−2.3...1.4)
OSU95	N (m)	5° × 5°	0.79 (−5.0...3.0)	0.35 (−3.4...1.8)
			0.76 (−6.3...2.4)	0.30 (−3.6...1.8)
Marsh 89*	Δg (mgal)	5° × 5°	4.3 (−21.3...19.7)	3.2 (−13.6...24.4)
			4.3 (−19.1...20.3)	3.1 (−14.0...19.4)
Gravimetry				
OSU89*	Δg (mgal)	5° × 5°	6.4 (−27.6...28.6)	5.7 (−27.1...31.0)
			6.5 (−26.4...30.3)	5.6 (−27.4...29.7)
Doppler/GPS-Levelling				
DGL90*	N (m)	point values	1.56 (n = 941)	1.11 (n = 843)
			1.52 (n = 936)	0.93 (n = 773)
Spher. harm. model				
JGM2-S	N (m)	5° × 5°	0.60 (−3.0...4,0)	
	Δg (mgal)	5° × 5°	2.2 (−11.4...13.1)	
JGM3				
	N (m)	5° × 5°		0.43 (−3.8...5.7)
	Δg (mgal)	5° × 5°		2.4 (−31.0...37.1)

Table 10. Orbit fit to tracking data

Satellites	Arc length	Type of data	GRIM4-S4	GRIM4-C4	JGM2S	JGM3
ERS1	5d	laser (cm)	8.3	7.7	11.8	10.8
		X-over (cm)	14.7	14.3	16.6	14.9
SPOT-2	3d	Doris (mm/s)	.58	.57	.58	.57
STARLETTE	7d	laser (cm)	12.8	12.5	11.8	12.0
STELLA	6d	laser (cm)	11.6	10.9	85.7*	14.1
TOPEX	4d	laser (cm)	4.6	4.4	4.8	4.7
		Doris (mm/s)	.55	.55	.55	.55
		X-over (cm)	9.5	9.5	9.5	9.5
	30h	GPS-SST (cm)	2.4	2.5	2.4	2.4
LAGEOS–1	10d	laser (cm)	4.9	4.8	5.9	5.9
LAGEOS–2	10d	laser (cm)	4.4	4.4	5.3	5.1

* no STELLA data included

– state vector
– drag (scaling factor once per day in general, once per 6 h for SPOT-2, once per 12 h for ERS-1)
– solar radiation (scaling factor once per arc)
– empirical along-track acceleration at the once per rev. period for SPOT-2, ERS-1 and TOPEX, constant for Lageos
– empirical cross-track acceleration at the once per rev. period for ERS-1 and TOPEX.

One should mention that all orbit computations were done in the GRIM4 software environment (reference system, tides...) which can make the fit optimistic when using a GRIM4 model. Nevertheless these results show a very homogeneous precision even between satellite-only models and combined models. Most of the discrepancies between the GRIM4 and JGM models are below the one centimetre level for range, and negligible for range rate data. Only STARLETTE orbits seem to be slightly better adjusted with JGM3, whereas STELLA and ERS-1 orbits show a better fit with the GRIM4 model.

6. Conclusion

A new general model of the Earth gravitational potential called GRIM4 has been elaborated jointly in a multi-year effort between German and French groups. The spherical harmonic expansion has been determined up to degree and order 72. A considerable progress was achieved as compared to the previous GRIM3 model. For example, more than one order of magnitude improvement has been obtained in the accuracy of the radial component of the orbits of the satellites ERS-1 and TOPEX/POSEIDON, which are now at the 10 cm and 2 cm level, respectively. The positioning of ground stations by the DORIS tracking system has been made possible at the 2 cm level. The GRIM4 gravity field model with its two versions GRIM4-S4 (based on satellite tracking data only) and GRIM4-C4 (combined with Earth surface data) can compete with recent solutions derived at the NASA Goddard Space Flight Center in Washington and at the Center for Space Research, University of Texas in Austin, when used in satellite orbit computation or in the determination of the sea surface topography. Indeed all these models are practically based on the same data gathered with a lot of cooperative efforts well coordinated at the international level regarding the launch of satellites as well as their tracking (Nerem 1995). Of course, each model has its own specificity from a development point of view, with its own characteristics and certainly its own systematic errors: it usually performs slightly better when used with the software with which it was determined.

When realizing the extreme complexity in the development of such models, the large amount of small forces involved and their parameterization, one appreciates how important it has been that the same kind of works could be performed in several centres. It is also of utmost importance that there does not exist significant differences between the models.

The improvement in this new generation of models is due to the main following factors:

- the use of new satellite orbits such as those of SPOT-2, TOPEX/POSEIDON, ERS-1, STELLA as well as the intensive use of STARLETTE and LAGEOS,
- the progress accomplished in satellite tracking (by laser, GPS, DORIS) in precision but mainly in orbit coverage - which for example enables the determination of empirical along-track accelerations,
- the better knowledge of the sea surface topography,
- the increase in the coverage of surface gravity data,
- the better algorithms developed over the years, and the capabilities of super computers.

Progress is very probably again possible by observing new satellites (such as GFZ-1), by using new tracking systems (such as PRARE), by improving non-gravitational force modelling, also by taking into account, in a more consistent way, the temporal gravity variations and relativity effects. However, it is of great importance to emphasize that a dedicated mission is mandatory to reach the mean and the short-wavelength parts of the gravity field. It is especially a crucial point in oceanography. From this point of view the withdrawal of the NASA/ESA ARISTOTELES project based on gradiometry and GPS is very unfortunate. New opportunities however exist based either on the satellite

to satellite tracking technique or on satellite gradiometry or on both. It is hoped that new international and cooperative efforts will again be supported very soon.

References

Anzenhofer M, Gruber T, Rentsch M (1995) Global high resolution mean sea surface based on ERS-1 35- and 168- day cycles and Topex data. Proceedings IAG Symposium G3 of IUGG General Assembly, Boulder.

Balmino G, Reigber Ch, Moynot B (1978) Le modèle de potentiel gravitationnel terrestre GRIM2: Détermination, évaluation. Ann Geophys 34: 55–78

Balmino G (1992) Orbital choice and the theory of radial orbit error for altimetry. In: Rummel R & Sanso F (eds), Satellite Altimetry in Geodesy and Oceanography, Springer-Verlag, pp 243–315

Barlier F, Berger C, Falin JL, Kockarts G, Thuillier G (1978) A thermospheric model based upon satellite drag data. Ann Geophys 34: 9–24

Basic T, Rapp RH (1992) Oceanwide prediction of gravity anomalies and sea surface heights using Geos-3, Seasat, and Geosat altimeter data and ETOPOSU bathymetric data. Rep. 416, Dept. of Geod. Sci. and Surv., Ohio State University, Columbus, Ohio

Bender P, Goad C (1979) Probable LAGEOS contributions to a worldwide geodynamics control network. In: The Use of Artificial Satellites for Geodesy and Geodynamics, Vol. II, pp 145–161

De Mets C, Gordon RG, Argus DF, Stein S (1991) Current plate motions. Geophys J Int 101

Feissel M, Guinot B (1988) A homogeneous series of the Earth rotation parameters based on all observing techniques, 1962–1987, ERP(BIH)87CO2. In: BIH Annual Report for 1987, D-179-D84, BIH, Paris, France

Gruber T, Massmann F-H, Reigber C (eds) (1993) ERS-1 D-PAF Global Products Manual. GeoForschungsZentrum Postdam

Haefner R, Martin R (1966) Data reduction. In: Lundquist CA, Veis G (eds), Geodetic Parameters for a 1966 Smithsonian Institution Standard Earth, Smiths. Astrophys Obs, Special Report 200, pp 43–62, Cambridge Mass

Heiskanen W, Moritz H (1967) Physical Geodesy. Freeman WH and Co (eds), San-Francisco

Herring TA (1988) In: BIH Annual Report for 1987. D106-D107, BIH Paris, France

Kaula W (1966) Theory of Satellite Geodesy. Blaisdale Press, Waltham, Mass

Kim J-H, Rapp RH (1990) The development of the July 1989 1°× 1° and 30' × 30' terrestrial mean free-air anomaly data base. Rep. 403, Dept. of Geod. Sci. and Surv., Ohio State University, Columbus, Ohio

Klokoćnik J (1985) Further comparisons of Earth gravity models by means of lumped coefficients. Bull Astron Inst Czecosl 36: 27–43

Levitus S (1982) Climatological Atlas of the World Ocean, NOAA Prof. Paper 13, 173, U.S. Govt Print. Off. Washington, DC

Le Provost C, Genco ML, Lyard F, Vincent P, Canceil P (1994) Spectroscopy of the world ocean tides from a finite element hydrodynamic model. J Geophys Res 99 C12, 24777–24797

Makedonskii L, Balmino G, Galazin VF, Kogan MG, McNutt MK, Fairhead JD (1994) Gravity field over the former Soviet Union mapped. EOS, 75, 40: 463–464

McCarthy DD (1992) IERS Standards. IERS Technical Note 13, Central Bureau of IERS, Observatoire de Paris

Marini JW, Murray CW (1973) Correction of laser range tracking data for atmospheric refraction of elevations above 10 degrees. Doc. X-591- 73–351, Goddard Space Flight Center, Greenbelt, Md

Melbourne W, Anderle R, Feissel M, King R, McCarthy D, Smith D, Tapley B, Vincente R (1983) Project MERIT standards. Circ. 167, U.S. Nav. Obs., Washington, DC

Minster JB, Jordan JH (1978) Present day plate motions. J Geophys Res 83: 5331–5354

Nerem RS, Lerch FJ, Marshall JA, Pavlis EC, Putney BH, Tapley BD, Eanes RJ, Ries JC, Schutz BE, Shum CK, Watkins MM, Chan JC, Klosko SM, Luthcke SB, Patel GB, Pavlis NK, Williamson RG, Rapp RH, Biancale R, Nouel F (1994) Gravity model development for TOPEX/POSEIDON: Joint Gravity Models 1 and 2. J Geophys Res 99, C12, Special Issue, 24421–24447

Nerem RS, Jekeli C, Kaula WM (1995) Gravity field determination and characteristics: retrospective and prospective. J Geophys Res 100, B8, 15053–15074

Rapp RH, Wang YM, Pavlis NK (1991) The Ohio State 1991 geopotential and sea surface topography harmonic coefficient models. Rep. 410, Dep. of Geod. Sci. and Surv., The Ohio State Univ., Columbus, Ohio

Rapp RH, Yi Y (1995) The OSU MSS 1995. Personnal communication and Poster paper at the SWT meeting, JPL

Reigber Ch (1981) Representation of orbital elements variations and force function with respect to various reference systems. Bull Geod 55, 2: 111–131

Reigber Ch, Balmino G, Moynot B, Mueller H (1983) The GRIM3 Earth gravity field model. Manuscripta Geodaetica 8: 93–138

Reigber Ch, Balmino G, Müller H, Bosch W, Moynot B (1985) GRIM gravity model improvement using LAGEOS (GRIM3-L1). J Geophys Res 90, B11, 9285-9299

Reigber Ch, Schwintzer P, Müller H, Barth W, Massmann F-H (1988) Earth rotation from laser ranging to LAGEOS, ERP (DGFII)87L02, station coordinates from laser ranging to LAGEOS, SSC (DGFII)87L03. BIH Annual Report for 1987, D57-D62, BIH, Paris, France

Reigber Ch (1989) Gravity field recovery from satellite tracking data. In: Sanso F and Rummel R (eds), Theory of Satellite Geodesy and Gravity Field Determination, pp 197–234, Springer, Berlin, Germany

Ricard Y, Vigny C, Froidevaux C (1989) Mantle heterogeneities; geoid and plate motion: Monte-Carlo inversion. J Geophys Res 94, B10, 17543–17559

Rosborough GW, Tapley B (1987) Radial, transverse and normal satellite position perturbations due to the geopotential. Celestial Mechanics 40: 409–421

Schwiderski EW (1980) On charting global ocean tides. Rev Geophys 18: 243–268

Schwintzer P (1990) Sensitivity analysis in least squares gravity field modelling by means of redundancy decomposition of stochastic a priori information. Internal report PS/51/90, DGFI, Dept. I, München, Germany

Schwintzer P, Reigber Ch, Massmann F-H, Barth W, Raimondo JC, Gerstl M, Li H, Biancale R, Balmino G, Moynot B, Lemoine JM, Marty JC, Boudon Y, Barlier F (1991) A new Earth gravity field model in support of ERS-1 and SPOT-2: GRIM4-S1/C1. Final report to the German and French Space Agencies (DARA and CNES). München/Toulouse

Stephens GL, Campbell GG, Von der Haar TH (1990) Earth radiation budgets. J Geophys Res 95, C3, 2887–2898

Tapley BD, Watkins MM, Ries JC, Davis GW, Eanes RJ, Poole SR, Rim HR, Schutz BE, Shum CK, Nerem RS, Lerch FJ, Pavlis EC, Klosko SM, Pavlis NK, Williamson RG (1994) The JGM-3 gravity model. Annales Geophysicae 12, Suppl.1, C192

Veis G (1960) Geodetic uses of artificial satelites. Smithsonian Contr Astrophys 3, N ° 9, 95–161